Chapter 5

Zeptogram Scale Nanomechanical Mass Sensing

Very high frequency nanoelectromechanical systems (NEMS) provide unprecedented sensitivity for inertial mass sensing. We demonstrate *in situ* measurements in *real time* with mass noise floor ~20 zeptogram. Our best mass sensitivity corresponds to ~7 zeptograms, equivalent to ~30 Xenon atoms or the mass of an individual 4 kDa molecule. Detailed analysis of the ultimate sensitivity of such devices based on these experimental results indicates that NEMS can ultimately provide inertial mass sensing of individual intact, electrically neutral macromolecules with single-Dalton (1 amu) sensitivity.

5.1 Introduction

Today mechanically based sensors are ubiquitous, having a long history of important applications in many diverse fields of science and technology. Among the most responsive are sensors based on the acoustic vibratory modes of crystals,[1,2] thin films,[3] and more recently, microelectromechanical systems (MEMS)[4,5] and nanoelectromechancial systems (NEMS).[6,7] Two attributes of NEMS devices—minuscule mass and high quality factor (Q)— provide them with unprecedented potential for mass sensing. This is revealed in our analysis in chapter 3 and demonstrated by recently achieved femtogram[6] and attogram resolution.[7] Attainment of zeptogram (1 zg=10^{-21} g) sensitivity shown herein opens many new possibilities; among them is directly "weighing" the inertial mass of individual, electrically neutral macromolecules.[8] Such sensitivity also enables the observation of extremely minute (statistical) mass fluctuations that arise from the diffusion of atomic species upon the surfaces of NEMS devices—processes that impose fundamental sensitivity limits upon nanoscale gas sensors (see section 4.6). As an initial step into these applications, we perform mass sensing experiments with gaseous species adsorbed on the NEMS surfaces at the zeptogram scale.

5.2 Experimental Setup

All the experiments are done *in situ* within a cryogenically cooled, ultrahigh vacuum apparatus with base pressure below 10^{-10} Torr. As shown in figure 5.1, a minute, calibrated, highly controlled flux of Xe atoms or N_2 molecules is delivered to the device surface by a mechanically shuttered gas nozzle within the apparatus.[9] The nozzle has an

orifice with a 100 μm diameter aperture, which is maintained at T=200 K by heating it with ~1 W of power to prevent condensation of the gas within the orifice and its supply line. Gas is delivered to this nozzle from a buffering chamber (volume V_C =100 cm^3 for the N_2 experiments, and 126 cm^3 for the Xe experiments), in turn maintained at temperature T_C = 300 K. Prior to the commencement of a run, this chamber is pressurized with the species to be delivered, then sealed to allow escape only through the nozzle. Thereafter, the rate of pressure decrease, $\dot{P}_C$, which is continuously monitored, is proportional to the total adsorbate delivery rate from the gas nozzle to the NEMS sensor, i.e., the number of incident atoms or molecules per unit time. The total number flux of gas atoms or molecules out of the nozzle in steady state is given by $\dot{N}_C = \dot{P}_C V_C / k_B T_C$.

Real-time mass sensing is enabled by the incorporation of NEMS device into a VHF frequency modulation phase-locked loop (FM PLL), described in section 4.4. With this measurement scheme, data are obtained from two separate sets of experiments involving different NEMS resonators: a first device (hereafter, **D133**) with a fundamental resonant frequency f_0~133 MHz having dimensions: 2.3 μm (L) x 150 nm (w) x 70nm (t), and a second (hereafter, **D190**) with f_0~ 190 MHz and dimensions 2.3 μm (L) x 150 nm (w) x 100 nm (t). Both are patterned from SiC epilayers[10] and exhibit a quality factor of Q =5000 in the temperature range of the present measurement.

For our experiment, the NEMS devices are maintained at high vacuum (~10^{-7} torr) at 300K for >1 day prior to mass accretion studies. The experiments are carried out immediately after cryogenically cooling the devices in a background pressure below ~10^{-10} torr. Hence we assume the arriving species adsorb with unity sticking probability;

for our choices of Xe and N_2 this is a reasonable assumption.[11] The mass deposition rate to the device is then

$$\dot{M}_D = m\dot{N}_D = mA_D\,\dot{N}_C/(\pi L_D^{\,2}), \tag{5.1}$$

where m is the mass of adsorbed species (m_{Xe}=131 amu, m_{N_2}=28 amu), the factor A_D/L^2 is the solid angle of capture, A_D is the surface area of the device exposed to the flux, and L_D is the distance between the device and nozzle.[9] The weighting factor $1/\pi$ accounts for the cosine distribution of the beam profile. For N_2 experiment, $\dot{N}_C$ = 2.25 x 10^{12} molecules/sec, L_D = 2.37 cm, and A_D = 3.45 x 10^{-13} m^2, yielding $\dot{M}_D$=20.5 zg/sec. For the Xe experiment, the setting are $\dot{N}_C$ = 2.81 x 10^{12} atoms/sec, L_D=1.86 cm, and A_D=3.45x10^{-13} m^2. These values yield $\dot{M}_D$ = 195 zg/sec.

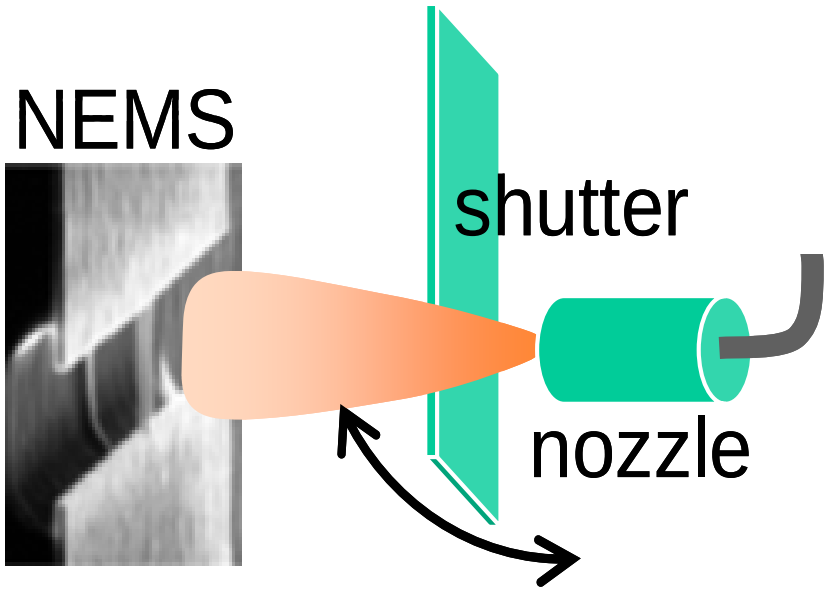

Figure 5.1. Experimental configuration. A gas nozzle with a 100 μm aperture provides a controlled flux of atoms or molecules. The flux is gated by a mechanical shutter to provide calibrated, pulsed mass accretions upon the NEMS device. The mass flux is determined by direct measurements of the gas flow rate, in conjunction with effusive-source formulas for the molecular beam emanating from the nozzle.

5.3 Mass Sensing at Zeptogram Scale

We first demonstrate the *real time*, *in situ*, zeptogram-scale mass accretion on **D190**, resulting from pulsed delivery of N_2 molecules at T=37 K, as shown in figure 5.2. With a mass deposition rate $\dot{M}_D$ = 20.5 zg/sec, sequential openings of the shutter for 5 second intervals provides a series of 100 zg accretions. The resulting discretely stepped frequency shifts tracked by the FM PLL confirm sequential, regular steps of mass accretion (each ~100 zg, i.e., ~2000 N_2 molecules).[12] The mass sensitivity δM is set by the standard deviation of frequency fluctuations on the plateaus

$$\delta M = \delta f / \Re = \left\langle (f - f_0)^2 \right\rangle^{1/2} / \Re . \qquad (5.2)$$

Here $\Re = \left| \partial f_0 / \partial M_{eff} \right|$ is the mass responsivity of the device; M_{eff} and f_0 are the effective vibratory mass and resonant frequency of the device, respectively. The data of figure 5.2 demonstrate δM =20 zg for the 1 sec averaging time employed.

The mass responsivities for the devices are directly determined from such pulsed atom or molecule deposition measurements. Data are shown both for **D190** (for conditions described above) and for **D133** in figure 5.3. We expose **D133** to Xe with mass deposition rate $\dot{M}_D$=195 zg/sec and opening shutter for 1 sec yields ~200 zg mass accretion (or equivalently ~900 Xe atoms) per data point at T =46 K. Both devices demonstrate unprecedented responsivities: $\Re$, directly extracted from the slope of the linear fit, at the level of roughly 1 Hz shift per zeptogram of accreted mass. More precisely, we find $\Re_{D133} \approx 0.96$ Hz/zg and $\Re_{D190} \approx 1.16$ Hz/zg. These values are in excellent agreement with the theoretical estimates from the expression $\Re \approx f_0 / 2M_{eff}$,

which yields ~0.89 Hz/zg for **D133** (M_{eff} ≈73 fg) and ~0.99 Hz/zg for **D190** (M_{eff} ≈96 fg).[8]

Our highest mass sensitivity, at present, is demonstrated with **D133** stabilized at T= 4.2 K. Exceptionally small fractional frequency fluctuations $\delta f / f_0 = \left\langle (f - f_0)^2 \right\rangle^{1/2} =$ 5×10^{-8} (50 ppb) are observed over a course of ~4000 sec interval with 1 sec averaging time (right inset of figure 5.3). This demonstrates attainment of a mass sensitivity of δM ~7 zg, equivalent to accretion of ~30 Xe atoms or, alternatively, of an *individual* 4 kDa macromolecule. Using M_{eff} ≈73 fg, Q~5000, and dynamic range DR ~80 dB, such a mass sensitivity is consistent with the estimated value 2.9 zg from the expression,

$$\delta M \sim (2M_{eff} / Q)10^{-DR/20}, \tag{5.3}$$

as described by Ekinci et al.[7] Our current dynamic range is determined, at the bottom end, by the noise floor of the posttransducer readout amplifier of the NEMS device and, at the top end, by the onset of nonlinearity arising from the Duffing instability for a doubly clamped beam (see section 3.2). With our current experimental setup, we are able to track mass accretions up to a total of ~2.3x10^6 Xe atoms on **D190**, with no observable change in the quality factor (see section 4.6). This confirms a remarkably large mass dynamic range from a few kDa (or several zeptogram sensitivity) up to ~100 MDa range, corresponding to almost femtogram-scale accretions.

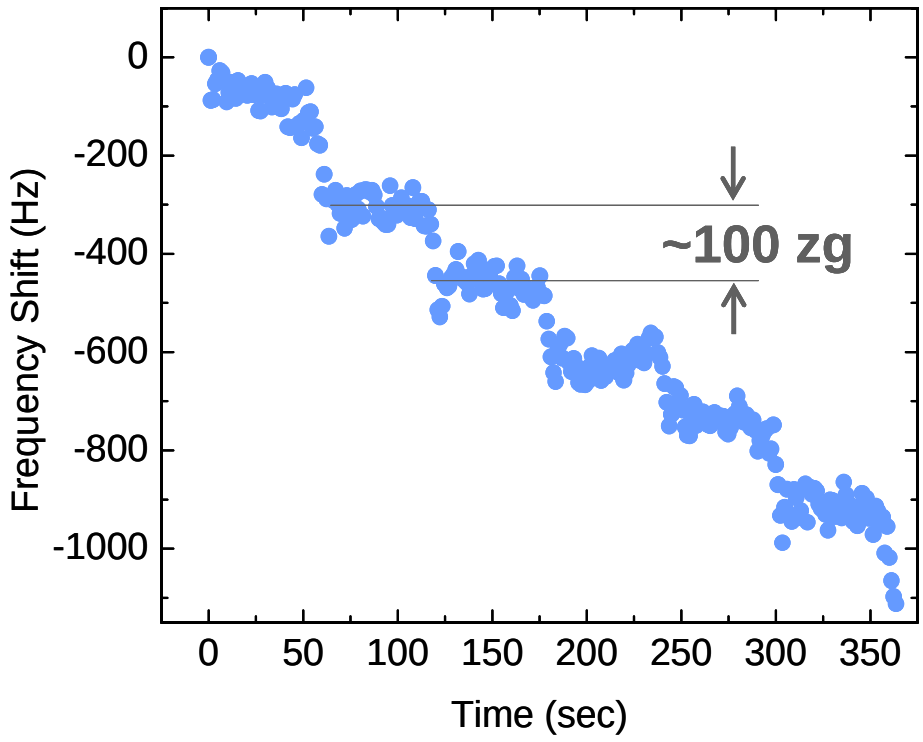

Figure 5.2. Real time zeptogram-scale mass-sensing experiment. Sequential mass depositions are executed *in situ* upon the 190 MHz device within a cryogenic UHV apparatus. The resulting frequency shift of the NEMS device is tracked in *real time* by a very high frequency (VHF) phase-locked loop. Each step in the data corresponds to a ~100 zg mass accretion (~2000 N_2 molecules) resulting from opening the mechanical shutter for 5 sec. The root-mean-square frequency fluctuations of the system correspond to a mass sensitivity of δM = 20 zg for the 1 sec averaging time employed.

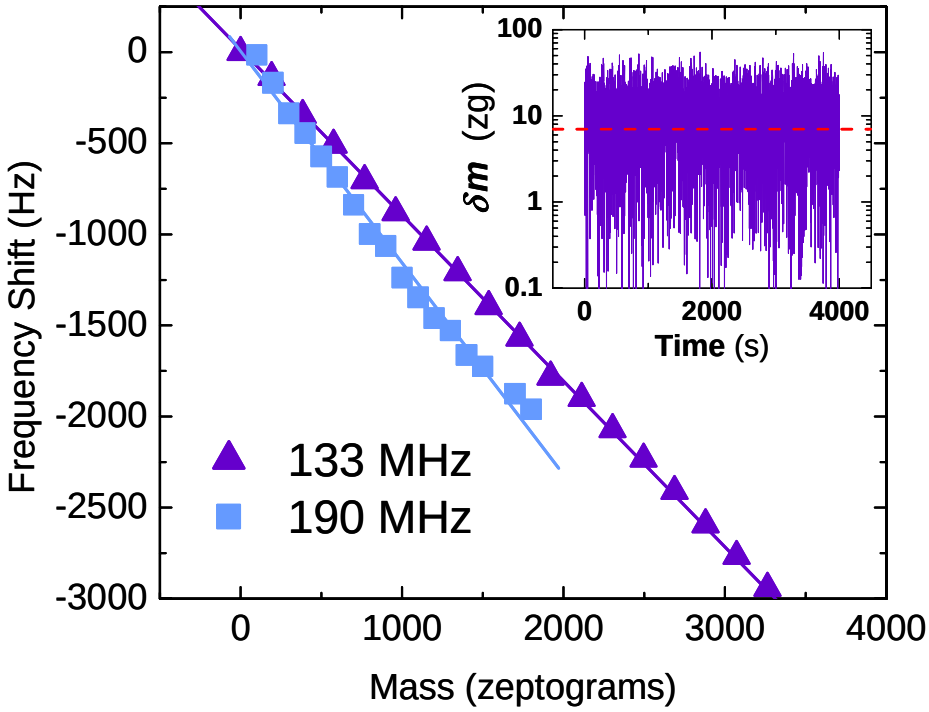

Figure 5.3. Mass responsivities of nanomechanical devices. The mass responsivities (resonant frequency shifts versus accreted mass) are measured for two VHF NEMS devices (operating at 133 MHz and 190 MHz). Xe atoms are accreted at T=46 K upon the 133 MHz device with ~200 zg mass increments per data point (purple). N_2 molecules are accreted at T=37 K upon the 190 MHz device with ~100 zg mass increments per data point (blue). The slopes of the mass loading curves directly exhibit the unprecedented mass responsivity on the order 1 Hz per zeptogram. **(right inset) Mass sensitivity.** The "mass noise floor" for the 133 MHz device, which originates from its frequency-fluctuation noise, is measured with 1 sec averaging time over the course of ~4000 sec while it is temperature stabilized at 4.2 K with zero applied flux. The average root-mean-square value (red dashed line), reflects the attainment of ~7 zg (i.e., ~4 kDa) mass sensitivity, the equivalent of ~30 Xe atoms.

5.4 Conclusion

We demonstrate NEMS mass sensing at the zeptogram scale. The agreement between predicted and experimentally observed values for both $\Re$ and δM confirms our analyses in chapter 3 and validates their use in projecting a path toward single-Dalton mass sensitivity.[8] Attainment of this goal is possible, for example, with a device having a fundamental resonant frequency of 1 GHz, vibratory mass of M_{eff}=1x10^{-16} g, and Q=10,000, using a transduction-readout system providing DR=80 dB. These are realistic parameters for next generation NEMS.[13] Huang, et al. recently attained NEMS vibrating in fundamental mode at microwave frequencies.[13] In conjunction with the recent development of techniques for improved Q,[14] and the advances in frequency-shift readout in the tens of ppb range, it is clear that NEMS sensing at the level of ~1 Da will soon be within reach. Attainment of NEMS mass sensors with single-Dalton sensitivity will make feasible the detection of *individual*, intact, electrically neutral macromolecules with masses ranging well into the hundreds of MDa range. This is an exciting prospect — when realized it will blur the traditional distinction between inertial mass sensing and mass spectrometry. We anticipate that it will also open intriguing possibilities in atomic physics and life science.[15,16]

References

1. D. S. Ballantine et al. *Acoustic Wave Sensors* (San Diego, Academic Press, 1997).

2 C. Lu *Application of Piezoelectric Quartz Crystal Microbalance* (London, Elsevier, 1984).

3. M. Thompson and D. C. Stone *Surface-Launched Acoustic Wave Sensors: Chemical Sensing and Thin Film Characterization* (New York, John Wiley and Sons, 1997).

4. J. Thundat, E. A. Wachter, S. L. Sharp, and R. J. Warmack Detection of mercury vapor using resonating microcantilevers. *Appl. Phys. Lett.* **66**, 1695–1697 (1995).

5. Z. J. Davis, G. Abadal, O. Kuhn, O. Hansen, F. Grey, and A. Boisen Fabrication and characterization of nanoresonating devices for mass detection. *J. Vac. Sci. Technol.* **B 18**, 612-616 (2000).

6. N. V. Lavrik and P. G. Datskos Femtogram mass detection using photothermally actuated nanomechanical resonators. *Appl. Phys. Lett* **82**, 2697 (2003).

7. K. L. Ekinci, X. M. H. Huang, and M. L. Roukes Ultrasensitive nanoelectromechanical mass sensing. *Appl. Phy. Lett.* **84**, 4469 (2004).

8. K. L. Ekinci, Y. T. Yang, and M. L. Roukes Ultimate limits to inertial mass detection based upon nanoelectromechanical systems. *J. Appl. Phys.* **95**, 2682 (2004).

9. H. Pauly and G. Scoles (editor) *Atomic and Molecular Beam Methods* (New York, Oxford University Press, 1988).

10. Y. T. Yang et al. Monocrystalline silicon carbide nanoelectromechancial systems. *Appl. Phys. Lett.* **78**, 162-164 (2001).

11. H. J. Kreuzer and Z. W. Gortel *Physisorption Kinetics* (Springer-Verlag, New York, 1986). At low coverage, unity sticking probability are observed for Xe on W(100) at T= 65 K. Xe on Ni(100) at T=30 K and N_2 on Ni(110) T=87 K. We expect the above to be representative materials and conditions, so that cryogenic adsorption upon the NEMS device will behave similarly in our case.

12. We have also verified that the arriving species provide negligible thermal perturbation upon the device. This is accomplished by high-resolution *in situ* resistance thermometry upon the metallic displacement-transducer electrode, and comparing shutter-open and shutter-closed conditions. The kinetic energy of the arriving species negligibly perturbs the device.

13. X. M. H. Huang, C. A. Zorman, M. Mehregany, and M. L. Roukes Nanodevices motion at microwave frequencies. *Nature* **421**, 496 (2003).

14. X. M. H. Huang, X. L. Feng, C. A. Zorman, M. Mehregany, and M. L. Roukes Free free beam silicon carbide nanomechanical resonators. *New J. Phys.* **7**, 247 (2005).

15. W. Hansel, P. Hommelhoff, T. W. Hansh, and J. Reichel Bose-Einstein condensation on microelectronic chips. *Nature* **413**, 498-500 (2001).

16. R. Aebersold and M. Mann Mass spectrometry-based proteomics. *Nature* **422**, 198-207 (2003).